



HAL
open science

Crustal loading in vertical GPS time series in Fennoscandia

Maaria Nordman, Jaakko Mäkinen, Heikki Virtanen, Jan M. Johansson,
Mirjam Bilker-Koivula, Jenni Virtanen

► **To cite this version:**

Maaria Nordman, Jaakko Mäkinen, Heikki Virtanen, Jan M. Johansson, Mirjam Bilker-Koivula, et al.. Crustal loading in vertical GPS time series in Fennoscandia. *Journal of Geodynamics*, 2009, 48 (3-5), pp.144. 10.1016/j.jog.2009.09.003 . hal-00594425

HAL Id: hal-00594425

<https://hal.science/hal-00594425>

Submitted on 20 May 2011

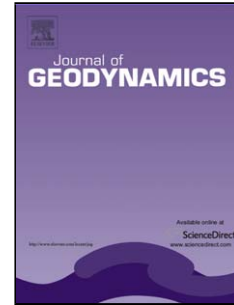
HAL is a multi-disciplinary open access archive for the deposit and dissemination of scientific research documents, whether they are published or not. The documents may come from teaching and research institutions in France or abroad, or from public or private research centers.

L'archive ouverte pluridisciplinaire **HAL**, est destinée au dépôt et à la diffusion de documents scientifiques de niveau recherche, publiés ou non, émanant des établissements d'enseignement et de recherche français ou étrangers, des laboratoires publics ou privés.

Accepted Manuscript

Title: Crustal loading in vertical GPS time series in Fennoscandia

Authors: Maaria Nordman, Jaakko Mäkinen, Heikki Virtanen, Jan M. Johansson, Mirjam Bilker-Koivula, Jenni Virtanen



PII: S0264-3707(09)00070-2
DOI: doi:10.1016/j.jog.2009.09.003
Reference: GEOD 897

To appear in: *Journal of Geodynamics*

Please cite this article as: Nordman, M., Mäkinen, J., Virtanen, H., Johansson, J.M., Bilker-Koivula, M., Virtanen, J., Crustal loading in vertical GPS time series in Fennoscandia, *Journal of Geodynamics* (2008), doi:10.1016/j.jog.2009.09.003

This is a PDF file of an unedited manuscript that has been accepted for publication. As a service to our customers we are providing this early version of the manuscript. The manuscript will undergo copyediting, typesetting, and review of the resulting proof before it is published in its final form. Please note that during the production process errors may be discovered which could affect the content, and all legal disclaimers that apply to the journal pertain.

1 **Crustal loading in vertical GPS time series in Fennoscandia**

2

3 Maaria Nordman* (1), Jaakko Mäkinen (1), Heikki Virtanen (1), Jan M. Johansson
4 (2), Mirjam Bilker-Koivula (1), Jenni Virtanen (1)

5

6 1 Finnish Geodetic Institute, Geodeetinrinne 2, P.O. Box 15, 02431 Masala, Finland

7 2 Chalmers University of Technology, Onsala Space Observatory, Sweden.

8 * Corresponding author, Maaria.Nordman@fgi.fi, tel. +358 9 29555216, Fax +358 9
9 29555211

10

11 Abstract

12 We compare time series of vertical position from GPS with modelled vertical
13 deformation caused by variation in continental water storage, variation in the level of
14 the Baltic Sea, and variation in atmospheric pressure. Monthly time series are used.
15 The effect of continental water storage was calculated from three different global
16 models. The effect of non-tidal variation in Baltic Sea level was calculated using tide
17 gauge observations along the coasts. Atmospheric loading was computed from a
18 numerical weather model. The loading time series are then compared with three
19 different GPS time series at seven stations in Fennoscandia. A more detailed analysis
20 is computed at three coastal stations. When the monthly GPS time series are corrected
21 using the load models, their root-mean-square scatter shows an improvement between
22 40 and zero percent, depending on the site and on the GPS solution. The modelled
23 load effect shows a markedly seasonal pattern of 15 mm peak-to-peak, of which the
24 uncorrected GPS time series reproduce between 60 and zero percent.

25

26 Keywords: crustal loading, Baltic Sea, atmospheric pressure, continental water, GPS

27 **Introduction**

28 The geographical distribution of atmospheric, oceanic and hydrologic masses varies in
29 time and this in turn loads and deforms the surface of the solid Earth. Such
30 deformations can be detected by GPS. Height changes due to atmospheric loading
31 were pointed out in global time series of GPS coordinates by van Dam et al. (1994).
32 The deformation due to variable loading by continental water storage was found by
33 van Dam et al (2001). Blewitt et al. (2001) demonstrated that a global mode of
34 seasonal mass exchange between the Northern and Southern hemisphere is detectable
35 in GPS data.

36
37 Many of the mass fluxes that produce the deformation follow a near-annual cycle. In
38 fact, time series of GPS positions typically show a seasonal variation, which is
39 tempting to associate with geophysical loads. However, Dong et al. (2002) estimated
40 that only about 40% of the seasonal power of apparent vertical motion could be
41 attributed to modelled mass redistribution. Similarly, e.g. van Dam et al (2007) found
42 large discrepancies between seasonal vertical displacements estimated from GRACE
43 and observed at European GPS sites. The discrepancies are believed to be due to
44 technique errors and unmodelled or mismodelled factors in the GPS analysis.
45 Candidates for producing spurious long-period signals in the GPS time series include
46 the propagation of unmodelled short-period signals like tides to longer periods (Penna
47 and Stewart, 2003, Stewart et al., 2005, Penna et al., 2007, King et al. 2008),
48 mismodelling of troposphere delays (Munekane et al., 2008), the satellite repeat

49 constellation (Ray et al., 2008), monument movements, variation in local multipath
50 (Dong et al., 2002, Williams et al., 2004).

51

52 In this paper we investigate the agreement between GPS time series and independent
53 loading models in Fennoscandia, and the subsequent application of the models to
54 reducing GPS time series residuals. We compare time series of vertical positions from
55 GPS with modelled vertical deformation from three geophysical loads. They are the
56 atmospheric pressure variation, non-tidal variation in Baltic sea level, and continental
57 hydrology. The loads are studied at seven continuous GPS stations, five in Sweden,
58 one in Finland, and one in Norway (Figure 1a). We want to see whether the residuals
59 in the GPS time series can be reduced by the model corrections. We also compare the
60 seasonal pattern in GPS and in the load models. Our data on Baltic level is monthly,
61 as are the hydrology models. Therefore the GPS and atmospheric loading time series
62 are averaged to monthly means as well (see next chapter).

63 [Figure 1]

64 **Data and methods**

65 **GPS**

66 Figure 1a shows the positions of the 7 stations. We use three daily GPS time series of
67 vertical positions. Two of them are by M.B. Heflin and were obtained from the
68 Processing Centre of the International GNSS Service (IGS) at the Jet Propulsion
69 Laboratory (JPL) (<http://sideshow.jpl.nasa.gov/mbh/series.html>). These solutions
70 apply the no-fiducial strategy and GIPSY software. Daily solutions are aligned to the
71 ITRF2005 in the least-squares sense using either a 6-parameter (translation, rotation)
72 or 7-parameter (translation, rotation, scale) Helmert transformation. Hereafter we

73 refer to them as MHP6 and MHP7, respectively. The starting years for these time
74 series varies, from 1993 to 2004 depending on the station.

75

76 The third GPS time series is the one used for BIFROST studies (Johansson et al.,
77 2002). This is also calculated using the no-fiducial strategy and GIPSY. Satellite
78 orbits were referred to various releases of the International Terrestrial Reference
79 Frame ITRF. The geodetic positions were then transformed to a frame provided by M.
80 Heflin, using a core subset of the BIFROST stations; for description see Johansson et
81 al. (2002). We refer to this time series as JJ and the data span is 1993–2006 at all our
82 stations.

83

84 All time series use the same strategy, cut-off angle of 15° and IERS conventions for
85 the solid Earth tide and ocean tidal loading. The models of ocean tidal loading used in
86 GPS processing do not include Baltic tides. They are a few centimetres only, and thus
87 negligible in the terms of the load. The effect of non-tidal ocean loading for our
88 stations is small, 1.5-2 mm peak-to-peak from the ECCO-model (Takiguchi et al.
89 2006), and is neglected. At the (seasonal) timescales of interest here, the GPS time
90 series approximately refer to the CF (Center of Figure) frame (Dong et al., 2002).

91

92 Since the GPS time series show larger scatter in the beginning, we left the first years
93 out and chose a time period 1997-2006 (10 years) for all the stations, when available.

94 All daily series were decimated to monthly series taking the simple average over a
95 calendar month. The time series of all the stations are plotted in Figure 1b.

96 ***Baltic Sea***

97 We used monthly tide gauge (TG) data from all around the Baltic, provided by the
98 Permanent Service for Mean Sea Level (Woodworth and Player, 2003). The reference
99 for the sea level was determined by regression of the whole lengths of the TG records
100 and by fixing the epoch to 2000.5. Monthly series of a sea surface model were created
101 using the minimum-curvature-surface interpolation scheme with splines (Smith and
102 Wessel, 1990). The number of available TG stations varies monthly, between 22 and
103 26, but the interpolation scheme is not sensitive to missing support points. The
104 loading deformation was calculated from these sea-surface models by convolving
105 them with the Green's function from the Gutenberg-Bullen Earth model (Farrell,
106 1972). The degree one Love numbers applied by Farrell (1972) imply that the frame is
107 CE (Center of mass of the solid Earth). For our purposes, the difference from CF
108 frame is negligible (Dong et al., 2002). Steric effects were neglected, i.e. sea heights
109 were equated with sea mass. For more details see Virtanen et al. (2008). An example
110 of a monthly Baltic Sea load deformation can be seen in Figure 1a.

111 ***Atmospheric loading***

112 We use the atmospheric pressure loading time series provided by the Goddard VLBI
113 group, available on the Web at <http://gemini.gsfc.nasa.gov/aplo/>. They were computed
114 by convolving the Green's function from the Preliminary Earth Model (PREM) with a
115 surface pressure field (Petrov and Boy, 2004). The surface pressure field comes from
116 the NCEP/NCAR Reanalysis numerical weather model and has a 2.5 x 2.5 degree
117 spatial resolution and 6-hour temporal resolution. We averaged the 6-hour values to
118 monthly means. In this time series, oceans are assumed to have the inverse barometer
119 (IB) response, but semi-enclosed seas like the Baltic Sea are taken to be “dry land”,

120 which is consistent with the Baltic Sea load computation. The frame of the time series
121 is CM, i.e., Centre of Mass of the entire solid Earth plus load.

122 ***Continental water storage***

123 We used three monthly models of continental water storage. The model of the Climate
124 Prediction Centre (CPC, Fan and van den Dool, 2004) only contains soil moisture, but
125 its leaky-bucket model can hold 0.76 m of water and therefore is capable of partly
126 accounting for groundwater, too. Snowfall is modelled as liquid water and thus it may
127 exit from the model too fast. The WaterGAP Global Hydrology Model (WGHM; Döll
128 et al. 2003) and the LaDWorld Gascoyne (Milly and Shmakin, 2002) account for all
129 aspects of water storage: snow, soil moisture, groundwater. We have used each model
130 in the whole area where it is released. WGHM excludes the polar ice sheets but
131 LaDWorld and CPC cover them.

132

133 To compensate for the change in total continental water storage, we add or subtract a
134 uniform layer of water to/from the oceans. Thus the global water mass is conserved
135 but gravitational consistency (Clarke et al., 2005) is not implemented. The time series
136 of deformation are then calculated by convolving the global loads with the Green's
137 function from the Gutenberg-Bullen Earth model by Farrell (1972). The frame is CE
138 (cf. the Baltic Sea above).

139 **Results and discussion**

140 ***Time series plots***

141 In the following figures all loads are relative to a mean value and time series plots
142 have been detrended. An example of a monthly Baltic Sea load can be seen in
143 Figure 1a. The deformation decreases rapidly with growing distance from the sea.

144

145 Figure 2a shows the monthly time series at Metsähovi: GPS, loading, and GPS
146 residuals after removing all loads. Figures 2b, 2c and 2d show the same time series at
147 Kiruna, Mårtsbo and Onsala, but with Metsähovi subtracted. Obviously, at closeby
148 stations the loading signals are very similar. However, at longer distances clear
149 differences already emerge, e.g. in the hydrological loading between Kiruna and
150 Metsähovi. Noteworthy are also the relatively large discrepancies between the
151 different hydrological models. The plots for Borås (not shown) are rather similar to
152 Onsala and Tromsö (not shown) resembles Kiruna.

153

154 As we are particularly interested in loading by the Baltic Sea, we have chosen three
155 stations for closer analysis: Metsähovi, Mårtsbo, and Visby. At the other stations its
156 loading is small.

157 [Figure 2]

158 ***Load time series as corrections to GPS***

159 Here we look at the load time series as corrections to GPS. We have computed the
160 standard deviations of the three GPS time series before and after the load effects in
161 various combinations have been corrected for. The standard deviations of the
162 individual load effects are given, too. This is done for the Visby station in Table 1, for
163 Mårtsbo in Table 2, and for Metsähovi in Table 3. We have then calculated the
164 reduction in the standard deviation with respect to the original GPS time series. The
165 change is expressed in percent and is negative if the standard deviation decreases, i.e.
166 improves. Note that for Visby and Mårtsbo the GPS time series MHP6 and MHP7
167 have only three years of data and for comparison also three-year period has been
168 computed for JJ solution (JJS). All the other GPS time series cover the period January

169 1997 to December 2006. Tables 1, 2 and 3 show that the performance of the
170 corrections depends on the site and on the GPS time series in question, both on its
171 length and on the solution (JJ or MH).

172 [Table 1]

173 [Table 2]

174 [Table 3]

175 At Visby the Baltic Sea correction reduces the standard deviation in all time series, for
176 MH time series also the hydrology correction helps. For the three-year time series at
177 Mårtsbo the hydrology models and Baltic Sea correction reduce the standard deviation
178 using almost every combination, whereas the ten-year time series (JJ) for the same
179 stations hardly improve. At Metsähovi the highest reductions are achieved in MHP6
180 using hydrology correction only.

181

182 The ten-year series MHP7 and JJ at Metsähovi respond almost identically to the
183 corrections, similarly the three-year series MHP7 and JJS at Mårtsbo. In fact this
184 could be expected as the GPS time series themselves (Fig 1a) are very similar. At
185 Visby the three-year series MHP7 and JJS differ appreciably in the winter 2006
186 (Fig 1a) and so does their response to the load corrections.

187

188 In nearly all instances, the hydrological time series improve MHP7 less than they do
189 MHP6. The difference between the MHP6 and MHP7 is that in the latter series a scale
190 parameter is included in the alignment to ITRF2005. Possibly the global fit for scale
191 couples into the global seasonal deformation cycle due to hydrology. The ten-year
192 series JJ show hardly any improvement from corrections, anywhere. Scherneck et al.
193 (2003) have discussed in detail the low admittance of load series into the GPS

194 observations in the shorter daily version of the series (Johansson et al., 2002), using a
195 much larger set of stations.

196

197 The relative performance of the different hydrological models depends on the station
198 and on the time series, no clear pattern emerges. The correction for the Baltic level
199 (“bs”) only works at Visby, which is situated in the middle of the Baltic Sea and also
200 near the coast. This is baffling as it is relatively large at all three stations. The poor
201 performance of the atmospheric correction (“aplo”) may be in part related to the fact
202 that our correction is in CM frame while the other time series are approximately in the
203 CF frame. We thus neglect the geocenter motion (motion of the CM relative to CF)
204 due to the atmosphere, which is at the monthly timescale is of the order 3 mm (e.g.,
205 Feissel-Vernier et al., 2006) which in turn is as large as our atmospheric correction in
206 the CM frame. On the other hand, Tregoning and van Dam (2005) show that there are
207 several sites where the correction for atmospheric loading does not improve GPS
208 daily series even when both are in the same frame.

209

210 The largest reductions in the GPS residuals are 20–40%, for the MHP7 and MHP6
211 series. This is similar to the results by Tervo et al. (2006) but the difference is that
212 they reached best results by removing all the loading factors.

213 ***Influence of load corrections on trend determination***

214 All our stations are in the area of the Fennoscandian postglacial rebound and it is of
215 interest to see how the load corrections influence the trend determination from the
216 GPS time series. Obviously, the formal uncertainty of the trend fitted using least
217 squares will decrease in the same way as the residual standard deviation in Tables 1,
218 2, and 3. But what about the trend itself? Table 4 gives the results of trend

219 determination for the three stations. There is the GPS time series name and the time
220 period for which the trend was computed, the trend from daily values and the trend
221 from monthly values. As could be expected, the values are quite similar, since the
222 same data set is used. The rest of the columns show the trends computed for the
223 different loading signals. The last three columns show the sum of the trends using
224 different hydrological models. The figures give the opposite number of the change in
225 the trend of the GPS time series, if it were corrected for the corresponding load(s).
226 Most of the trends are small as expected

227 [Table 4]

228 The hydrological models are not constructed for determination of hydrological long-
229 term trends but rather for the annual cycle and for short-term inter-annual phenomena.
230 They could perhaps be trusted only over a few years. However, we see that in Visby
231 and Mårtsbo, where the uncertain trends from the short 3-year GPS time series deviate
232 appreciably from the 10-year GPS trend, the inclusion of the hydrological load would
233 only make the discrepancy worse. On the contrary, the modelled loads with the
234 exception of the CPC seem near trend-free over the 10-year period.

235 ***Seasonal variation in the GPS and in the loading time series***

236 As discussed in the Introduction, GPS time series often show seasonal variation; in
237 apparent positions load phenomena like hydrology are also seasonal in nature.
238 Inspection of Figure 2 shows a clear seasonal signal in the hydrological time series,
239 and in the Metsähovi GPS series. For better visualization, we stack the GPS and load
240 time series for each site by averaging over each month separately. This simple method
241 has the advantage that no functional form (e.g. sinusoidal) is assumed for the
242 phenomena. The results are depicted in Figure 3. It shows the total load effect (in

243 which hydrology is represented by WGHM) and the three different GPS time series
244 for each station,

245 [Figure 3]

246 First note is that the load stacks are very similar at all stations and over both 10 and 3
247 years. In Metsähovi all time series are stacked over 10 years. The phases of the GPS
248 stack agree and are rather close to the phases of the load stack. The GPS amplitudes
249 are 40–80% of the load amplitude. JJ and MHP7 are near-identical as previously
250 noted. For Mårtsbo and Visby we use load stacks over 3 years and 10 years. GPS
251 stacks MHP6 and MHP7 are over 3 years and JJ over 3 and over 10 years. At Mårtsbo
252 the 3-year GPS stacks agree quite well. The amplitude of the JJ solution is not as clear
253 as for MHP6 and MHP7 but they all agree with the load. The 10-year JJ stack deviates
254 considerably from the load and shows only a very subdued annual cycle. At Visby,
255 the (3-year) MHP6 and MHP7 reproduce the phases of the load stack but have about
256 70 percent of its amplitude. The 3-year JJ stack is bimodal due to the data of the
257 winter 2006. The 10-year JJ stack does not show any seasonal pattern at all.

258

259 While at some stations the similarity of the annual cycle from GPS and from the load
260 models is obvious, it should be remembered that even at them the GPS seasonal
261 component explains only a part of the variation in the monthly GPS time series. E.g.
262 at Metsähovi subtracting the monthly means from the MHP6, MHP7, and JJ time
263 series decreases their standard deviation by 24, 11, and 5 percent, respectively. For the
264 3-year series at Mårtsbo the figures are 39, 5, and 5 percent. At Visby we have 13, –
265 18 and –18 percent, i.e. partly a deterioration. This is because we have taken into
266 account that in eliminating the monthly means the degrees of freedom decrease by 11.

267 **Conclusions and outlook**

268 We have studied the effect of the atmospheric pressure loading, the effect of the non-
269 tidal Baltic Sea loading and the effect of continental water loading at seven GPS
270 stations in Fennoscandia. Despite this being a limited region, the loading signals are
271 far from identical: the Baltic loading is limited to the vicinity of the sea and across the
272 region differences appear also in the continental water loading. At three sites close to
273 the Baltic the loading time series were compared with apparent vertical movements
274 derived from GPS. Removing the computed loading from the GPS time series reduce
275 the standard deviation, but not for all series nor for all combinations of loads. The
276 maximum reduction was found to be 23% at Metsähovi, 43% at Mårtsbo and 34% at
277 Visby. This is of the same size as in our previous results (Tervo et al., 2006).

278
279 The three GPS time series studied use the same processing strategy but different
280 alignment to the reference frame. This is reflected in their relationship to the load time
281 series. The MHP6 does not use a scale parameter in the alignment and after correcting
282 for the loads performs better than the MHP7 that does. The 10-year JJ and MHP7
283 series are not significantly improved by the loading corrections on any of the stations,
284 but the corresponding 3-year series at Mårtsbo are. For control we computed the 3-
285 year series at Metsähovi and found the same results (not shown) as at Mårtsbo. This
286 could be related to the piecewise transformations used in the alignment to the frame.

287
288 The three time series of hydrological loads differ appreciably but the GPS series do
289 not show clear preference for any of them. Obviously, there is considerable
290 uncertainty the models involved. No such uncertainty should appear in our Baltic load

291 model and therefore it is baffling that it does not perform better for the GPS. We will
292 improve the atmospheric load series by including the corresponding geocentre motion.

293

294 At the three stations analyzed, removing the seasonal variation decreases the standard
295 deviation of the monthly GPS solutions by maximally 40 percent. The seasonal
296 variation in GPS tends to underestimate the seasonal variation in modelled load.

297

298 **Acknowledgments.** The calculations were done using programs NLOADF (soil
299 moisture and Baltic Sea loading, Agnew, 1997), Generic Mapping Tools version
300 3.4.2. (maps, Wessel and Smith, 1998) and R version 2.4.1 (analysis and figures, R
301 Development Core Team, 2006). This work was partly funded by the Academy of
302 Finland (decision number 117094).

303

304 **References**

305 Agnew, D.C., 1997. NLOADF: A program for computing ocean-tide loading, J.
306 Geophys. Res., 102, 5109-5110.

307

308 Blewitt, G., Lavallée, D., Clark P., Nurutdinov K, 2001. A new global mode of Earth
309 deformation: Seasonal cycle detected, Science, 294, 2342– 2345.

310

311 Clarke, P. J., Lavallée, D., Blewitt, G., van Dam, T., Wahr J. M., 2005. Effect of
312 gravitational consistency and mass conservation on seasonal surface mass loading
313 models, Geophys. Res. Lett., 32, L08306, doi:10.1029/2005GL022441

314

- 315 Döll, P., Kaspar, F., Lehner, B., 2003. A global hydrological model for deriving water
316 availability indicators: model tuning and validation. *J. Hydrol.* 270, 105-134.
317
- 318 Dong, D., Fang P., Bock Y., Cheng M. K., Miyazaki S., 2002. Anatomy of apparent
319 seasonal variations from GPS-derived site position time series, *J. Geophys. Res.*,
320 107(B4), 2075, doi:10.1029/2001JB000573.
321
- 322 Dong, D., Yunck, T., Heflin M., 2003. Origin of the International Terrestrial
323 Reference Frame, *J. Geophys. Res.*, 108(B4), 2200, doi:10.1029/2002JB002035
324
- 325 Fan, Y., van den Dool H., 2004. Climate Prediction Center global monthly soil
326 moisture data set at 0.5° resolution for 1948 to present, *J. Geophys. Res.*, 109,
327 D10102, doi:10.1029/2003JD004345.
328
- 329 Farrell, W.E., 1972. Deformation of the Earth by surface loads. *Rev. Geophys. Space*
330 *Phys.* 10, 761–797.
331
- 332 Feissel-Vernier, M., Le Bail, K., Berio, P., Coulot, D., Valette, J. 2006. Geocenter
333 motion measured with DORIS and SLR and predicted by geophysical models,,
334 *Journal of Geodesy*, 80, 637-648, DOI 10.1007/s00190-006-0079-z
335
- 336 Johansson, J.M., Davis J.L., Scherneck H.-G., Milne G.A., Vermeer M., Mitrovica
337 J.X., Bennett R.A., Elgered G., Elósegui P., Koivula H., Poutanen M., Rönnäng B.O.,
338 Shapiro I.I., 2002. Continuous GPS measurements of postglacial adjustment in

- 339 Fennoscandia, 1. Geodetic Results, J. Geophys. Res., Vol. 107, No. B8, DOI
340 10.1029/2001JB000400.
- 341
- 342 King, M. A., Watson, C. S., Penna, N. T., Clarke P. J., 2008. Subdaily signals in GPS
343 observations and their effect at semiannual and annual periods, Geophys. Res. Lett.,
344 35, L03302, doi:10.1029/2007GL032252.
- 345
- 346 Milly, P. C. D., Shmakin A. B., 2002. Global modeling of land water and energy
347 balances. part I: The Land Dynamics (LaD) model, J. Hydrometeorol., 3, 283– 299.
- 348
- 349 Munekane, H., Kuroishi, Y., Hatanaka Y. Yurai H., 2008. Spurious annual vertical
350 deformations over Japan due to mismodelling of tropospheric delays, Geophys. J. Int.
351 (2008) 175, 831–836 doi: 10.1111/j.1365-246X.2008.03980.x
- 352
- 353 Penna, N. T., Stewart M. P., 2003. Aliased tidal signatures in continuous GPS height
354 time series, Geophysical Research Letters, 30(23), 2184, doi:10.1029/2003GL018828.
- 355
- 356 Penna, N., King M., Stewart M., 2007. GPS height time series: Short period origins of
357 spurious long period signals, J. Geophys. Res., 112, B02402,
358 doi:10.1029/2005JB004047.
- 359
- 360 Petrov, L. Boy J.-P., 2004. Study of the atmospheric pressure loading signal in VLBI
361 observations, Journal of Geophysical Research, 10.1029/2003JB002500, Vol. 109,
362 No. B03405.
- 363

- 364 R Development Core Team, 2006. R: A language and environment for statistical
365 computing, R Foundation for Statistical Computing, Vienna, Austria. ISBN 3-
366 900051-07-0, URL <http://www.R-project.org>.
- 367
- 368 Ray, J., Altamimi, Z., Collilieux, X., van Dam, T., 2008. Anomalous harmonics in the
369 spectra of GPS position estimates. *GPS Solutions* 12, 55–64.
- 370
- 371 Scherneck H.-G., Johansson J.M., Koivula H., van Dam, T., Davis J.L., 2003. Vertical
372 crustal motion observed in the BIFROST project. *Journal of Geodynamics*, Vol 35,
373 No.4-5, pp.425-441
- 374
- 375 Smith, W.H.F. Wessel, P., 1990. Gridding with continuous curvature splines in
376 tension, *Geophysics*, 55, 293–305.
- 377 .
- 378 Stewart, M. P., Penna N. T., Lichti D. D., 2005. Investigating the propagation
379 mechanism of unmodelled systematic errors on coordinate time series estimated using
380 least squares, *J. Geod.*, 79, 479 – 489, doi:10.1007/s00190-005-0478-6.
- 381
- 382 Takiguchi, H., Otsubo, T., Fukuda, Y., 2006. Mass-redistribution-induced crustal
383 deformation of global satellite laser ranging stations due to non-tidal ocean and land
384 water circulation, *Earth, Planets and Space*, Volume 58, p. e13-e16.
- 385
- 386 Tervo M., Virtanen H., Bilker-Koivula M., 2006. Environmental loading effects on
387 GPS time series, *Bull. d’Inf. Marées Terr.* 142: 11407 – 11416.
- 388

389 Tregoning P., van Dam T., Atmospheric pressure loading corrections applied to GPS
390 data at the observation level, *Geophys. Res. Lett.*, 32, L22310,
391 doi:10.1029/2005GL024104, 2005.

392

393 van Dam, T., Blewitt G., Heflin M.B., 1994. Atmospheric pressure loading effects on
394 GPS coordinate determinations, *J. Geophys. Res.*, 99, 23939-23950.

395

396 van Dam, T., Wahr J., Milly P.C.D., Shmakin A.B., Blewitt G., Lavallée D., Larson
397 K.M., 2001. Crustal displacements due to continental water loading, *Geophysical
398 Research Letters*, 28, 651-654.

399

400 van Dam, T., Wahr J., Lavallée D., 2007. A comparison of annual vertical crustal
401 displacements from GPS and Gravity Recovery and Climate Experiment (GRACE)
402 over Europe, *J. Geophys. Res.*, 112, B03404, doi:10.1029/2006JB004335.

403

404 Virtanen, J., Mäkinen, J., Koivula-Bilker, M., Virtanen, H., Nordman, M., Kangas, A.,
405 Johansson, M., Shum, C.K., Lee, H., Wang L., Thomas, M., 2008. Baltic sea mass
406 variations from GRACE: comparison with in situ and modelled sea level heights.

407 Presented at the IAG International Symposium “Gravity, Geoid and Earth
408 Observation 2008” GGEO2008, Chania, Crete, 23–27 June 2008. In press.

409

410 Williams, S. D. P., Bock Y., Fang P., Jamason P., Nikolaidis R. M., Prawirodirdjo L.,
411 Miller M., Johnson D. J., 2004. Error analysis of continuous GPS position time series,
412 *J. Geophys. Res.*, 109, B03412, doi:10.1029/2003JB002741.

413

414 Wessel, P. Smith, W. H. F., 1998. New, improved version of Generic Mapping Tools
415 released, EOS Trans. Amer. Geophys. U., 79, 579

416

417 Woodworth, P., Player R., 2003. The Permanent service for mean seal level: an
418 update to the 21st century. J. of Coas. Res. 19(2), pp.287-295.

419

420

Accepted Manuscript

420 **Figure and table captions**

421

422 Figure 1. a) Loading caused by the Baltic Sea in March 2006 and the positions of the
423 GPS stations. The scale is in millimetres. b) The GPS time series of all the stations,
424 scale is in millimetres. TROM=Tromsö, KIRU=Kiruna, MART=Mårtsbo,
425 METS=Metsähovi, VISB=Visby, BORA= Borås, ONSA=Onsala. Solid black line =
426 JJ, gray line = MHP6, dashed black line = MHP7. The peaks in Kiruna ja Tromsö time
427 series are likely due to snow accumulation on top of the antenna.

428

429 Figure 2. Time series. a) Metsähovi b) difference Kiruna – Metsähovi (distance 880
430 km) c) difference Mårtsbo – Metsähovi (distance 410 km) d) difference Onsala –
431 Metsähovi (distance 790 km). The top panel (gps) is the GPS time series (or the
432 difference) after trend removal: solid black line = JJ, gray line = MHP6, dashed black
433 line = MHP7. The second panel from top (bs) is the Baltic Sea loading and the third
434 panel (ap) the atmospheric pressure loading. The fourth panel (cw) shows three
435 different continental water model loads: solid black line = CPC, gray line = WGHM,
436 dashed black line = LadWorld. The fifth panel shows the sum of the loads i.e. panels
437 2, 3 and 4. The bottom panel (resid) shows the GPS time series residual after the
438 loading time series are subtracted. The WGHM was used for water load. The different
439 lines are the same as for the top panel. The peaks in the Kiruna GPS time series are
440 due to snow accumulation on top of the antenna. The scale is in millimetres.

441

442 Figure 3. Stacked time series for stations Metsähovi, Mårtsbo and Visby. The monthly
443 mean for the whole time series has been computed and plotted. The circles show the
444 sum of the loading factors, the triangles show the JJ time series and the grey symbols

445 show the MH time series, plusses the 6-parameter transformation and crosses the 7-
446 parameter transformation. The dashed line is for 10-year time series of JJ and solid
447 line for 3-year in Mårtsbo and Visby.

448

449 Table 1. The results for station Visby, standard deviations in mm of the different time
450 series and their reduction with respect to the original time series. MH p6 = MH time
451 series with 6-parameter transformation, MH p7 = the same, but with 7 parameters, JJ
452 = BIFROST time series, JJS = JJ time series for 3 years, red % = reduction percentage
453 of the standard deviation, gps = GPS time series after trend removal, aplo =
454 atmospheric pressure loading, bs = Baltic Sea loading, wghm = continental water
455 loading from model WGHM, cpc = continental water loading from model CPC, ladw
456 = continental water loading from model LadWorld. The standard deviations of the
457 load time series (aplo, bs, wghm, cpc, ladw) are 2.73, 2.01, 3.91, 2.01, 0.80 mm (10
458 years) and 2.81, 2.19, 3.77, 1.70, 0.83 mm (3 years).

459

460 Table 2. The results for the station Mårtsbo. The abbreviations are the same as in
461 Table 1. The standards deviations of the load time series (aplo, bs, wghm, cpc, ladw)
462 are 2.72, 1.24, 4.23, 2.18, 1.68 mm (10 years) and 2.68, 1.34, 3.96, 1.82, 1.68 (3
463 years).

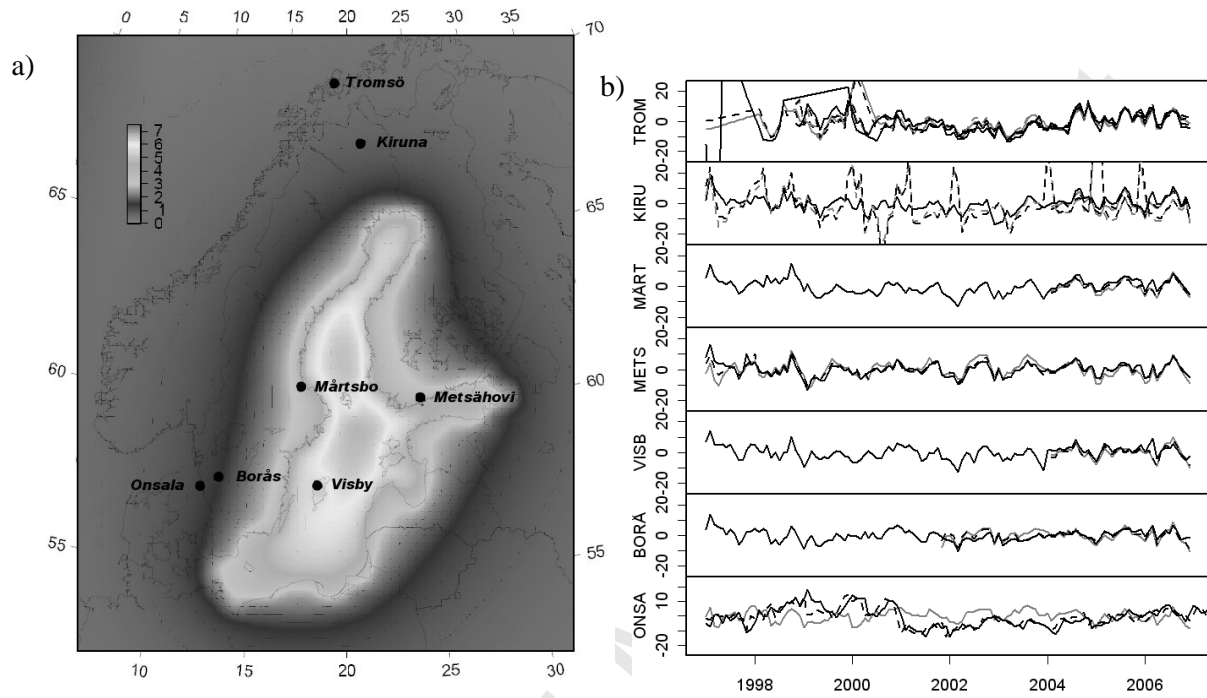
464

465 Table 3. The results for the station Metsähovi. The abbreviations are the same as in
466 Table 1. The standards deviations of the load time series (aplo, bs, wghm, cpc, ladw)
467 are 3.07, 1.38, 4.75, 2.27, 2.35 mm.

468

469 Table 4. The determined trends (mm/year) from different time series. The first
470 column gives the name of the GPS time series, MHp6 = MH time series with 6-
471 parameter transformation, MHp7 = the same, but with 7 parameters, JJ = BIFROST
472 time series, and their length (10 or 3 years). gps/d = trend determined from daily GPS
473 time series, gps /m = trend from the monthly time series, aplo = atmospheric pressure
474 loading, bs = Baltic Sea loading, wghm = continental water loading from model
475 WGHM, cpc = continental water loading from model CPC, ladw = continental water
476 loading from model LadWorld, sum (A) = the trend of the sum of the loadings using
477 different water models A.
478

478

479 **Figures**

480

481 Figure 1. a) Station positions and loading in millimetres for March 2006. b) GPS time

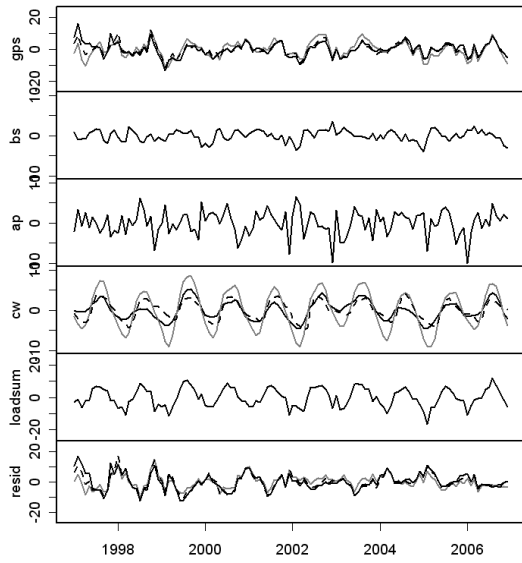
482 series.

483

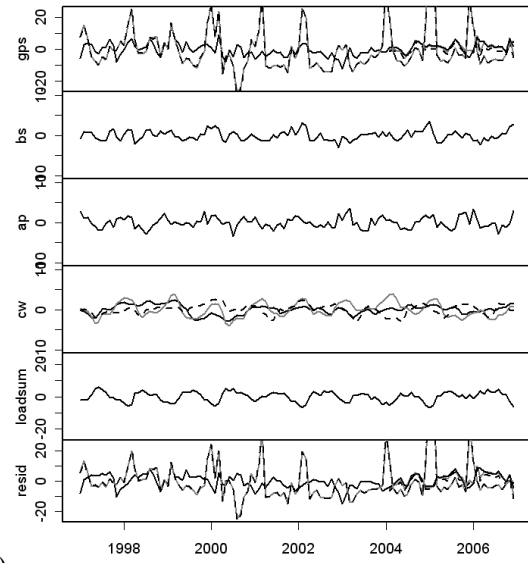
484

484

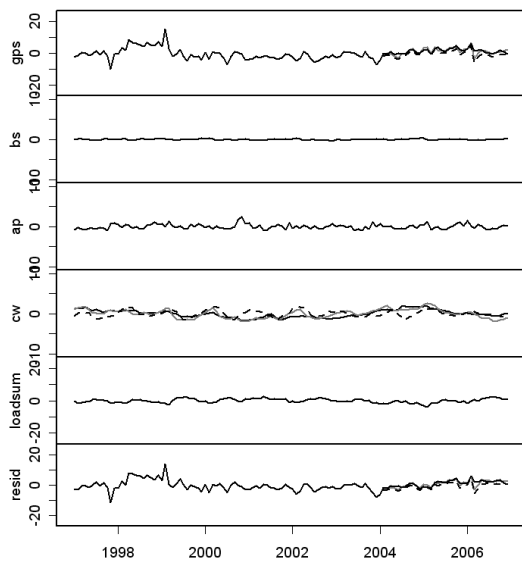
485 a)



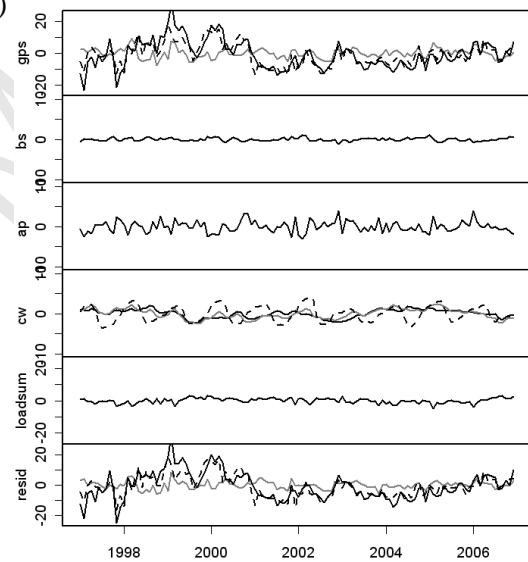
b)



c)



d)



486

487

488 Figure 2. Time series. a) Metsähovi b) difference Kiruna – Metsähovi c) difference

489 Märtsbo – Metsähovi d) difference Onsala – Metsähovi.

490

490

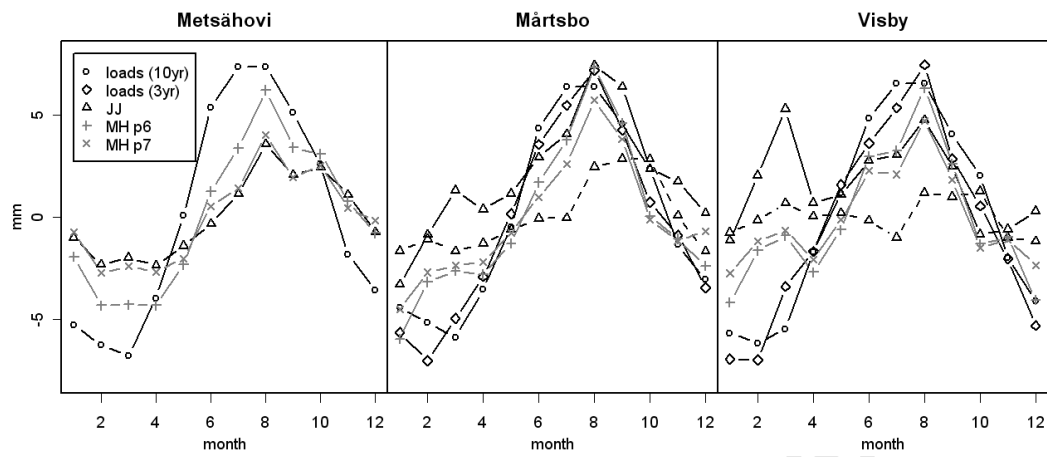
491
492
493
494
495

Figure 3. Stacked time series for all three stations.

495

496 **Tables**

497

498 Table 1. Results for Visby

499

VISBY	MHp6	red %	MHp7	red %	JJS (3-yr)	red %	JJ(10-yr)	red %
gps	4.22	0.0	3.61	0.0	3.22	0.0	4.38	0.0
- aplo	4.66	10.4	4.33	20.0	4.02	24.7	5.38	22.6
- bs	3.96	-6.3	3.34	-7.4	2.49	-22.7	4.05	-7.7
- wghm	3.47	-17.9	3.62	0.5	4.31	33.6	5.53	26.1
- cpc	3.28	-22.3	3.00	-16.9	3.13	-2.8	4.41	0.5
- ladw	3.85	-8.9	3.36	-6.8	3.10	-3.9	4.47	2.0
- aplo-bs	4.18	-1.1	3.85	6.6	3.14	-2.5	4.74	8.2
- aplo-wghm	4.60	9.0	4.91	36.1	5.44	68.7	6.54	49.2
- bs-wghm	2.78	-34.1	3.03	-16.0	3.50	8.7	5.36	22.2
- aplo-bs-wghm	3.85	-8.9	4.25	17.8	4.60	42.9	6.11	39.4
- aplo-bs-cpc	3.64	-13.7	3.70	2.4	3.50	8.5	4.95	12.9
- aplo-bs-ladw	3.81	-9.9	3.63	0.6	3.03	-6.0	4.82	9.9

500

501

502

502
503
504

Table 2. Results for Mårtsbo

MÅRTSBO	MHp6	red %	MHp7	red %	JJS (3-yr)	red %	JJ(10-yr)	red %
gps	4.05	0.0	3.29	0.0	3.41	0.0	4.65	0.0
- aplo	4.08	0.8	3.53	7.3	3.76	10.2	5.31	14.3
- bs	4.21	4.1	3.51	6.6	3.42	0.2	4.68	0.8
- wghm	2.29	-43.4	2.48	-24.5	2.61	-23.6	5.10	9.9
- cpc	2.58	-36.2	2.15	-34.8	2.35	-31.1	4.31	-7.3
- ladw	2.94	-27.3	2.40	-27.2	2.66	-22.1	4.61	-0.8
- aplo-bs	3.88	-4.1	3.32	0.8	3.35	-1.7	5.01	7.9
- aplo-wghm	3.22	-20.4	3.56	8.2	3.76	10.4	5.77	24.2
- bs-wghm	2.29	-43.3	2.51	-23.8	2.34	-31.3	5.19	11.6
- aplo-bs-wghm	2.73	-32.6	3.14	-4.7	3.15	-7.7	5.54	19.2
- aplo-bs-cpc	2.89	-28.7	2.79	-15.4	2.85	-16.5	4.79	3.1
- aplo-bs-ladw	2.89	-28.7	2.63	-20.1	2.77	-18.8	4.99	7.4

505
506
507

507 Table 3. Results for Metsähovi

508

METSÄHOVI	MHp6	red %	MHp7	red %	JJ	red %
gps	4.98	0.0	4.05	0.0	4.47	0.0
- aplo	5.50	10.6	4.76	17.4	5.15	15.1
- bs	5.01	0.6	4.19	3.4	4.58	2.4
- wghm	3.82	-23.2	4.45	10.0	4.95	10.7
- cpc	3.97	-20.3	3.65	-9.8	4.11	-8.1
- ladw	3.94	-20.8	3.68	-9.1	4.24	-5.2
- aplo-bs	5.17	3.8	4.46	10.0	4.85	8.5
- aplo-wghm	4.69	-5.7	5.28	30.5	5.74	28.2
- bs-wghm	4.01	-19.4	4.71	16.2	5.17	15.5
- aplo-bs-wghm	4.43	-11.1	5.13	26.7	5.58	24.8
- aplo-bs-cpc	4.40	-11.6	4.30	6.1	4.70	5.1
- aplo-bs-ladw	4.22	-15.2	4.17	2.9	4.68	4.7

509

510

511

511

512

Table 4. Trend determination

	mm/year	gps/d	gps/m	aplo	bs	wghm	cpc	ladw	sum (wghm)	sum (cpc)	sum (ladw)
METS	MHp6 (10yr)	5.48	5.43	-0.19	0.04	0.20	0.42	0.08	0.04	0.27	-0.07
	MHp7 (10yr)	5.61	5.58								
	JJ (10 yr)	5.48	5.45								
MART	MHp6 (3yr)	7.51	7.19	-0.17	0.06	0.58	0.80	0.27	0.48	0.70	0.17
	MHp7 (3yr)	7.85	7.68								
	JJ (3yr)	8.20	7.82								
	JJ (10 yr)	8.12	7.90	-0.17	0.03	0.17	0.50	0.01	0.03	0.36	-0.13
VISB	MHp6 (3yr)	2.03	1.46	-0.23	0.05	0.96	1.08	0.18	0.78	0.89	0.00
	MHp7 (3yr)	2.38	1.95								
	JJ (3yr)	3.33	3.14								
	JJ (10 yr)	3.56	3.78	-0.16	0.05	0.10	0.43	0.04	-0.01	0.31	-0.08

513

514